Journal of Applied Electrochemistry **29**: 693–702, 1999.

Oxidation–reduction processes in halide and oxohalide niobium containing melts. Part I: Interaction of fluoride–chloride and oxofluoride–chloride Nb(V) melts with niobium oxides

V.V. GRINEVITCH[1]*, V.A. REZNICHENKO[1], M.S. MODEL[1], S.A. KUZNETSOV[2], E.G. POLYAKOV[2] and P.T. STANGRIT[2]

[1]*Baikov Institute of Metallurgy and Materials Science, Russian Academy of Sciences, Leninskii prospect 49, 117911 Moscow, Russia;*

[2]*Institute of Chemistry, Kola Science Centre of the Russian Academy of Sciences, 184200 Apatity, Russia*

*(*author for correspondence, e-mail: grin@ultra.imet.ac.ru)*

Received 19 June 1996; accepted in revised form 2 December 1997

Key words: halide melts, niobium, niobium oxides, oxohalide melts

Abstract

The interaction between the K_2NbF_7–KCl–NaCl melt widely used for niobium electrolysis and niobium oxides of higher (Nb_2O_5) and lower (NbO_2 and NbO) oxidation states was studied by linear sweep voltammetry and analysis of the dissolution time dependences. Three monooxofluoride complexes, $NbOF_4^-$, $NbOF_5^{2-}$ and $NbOF_6^{3-}$, may form at the mole ratio of $Nb_2O_5 : K_2NbF_7 = 1 : 3$. No significant difference was found in the electrochemical behaviour of the complexes, but their discharge potentials become more negative with increasing number of fluorine anions in the complex. Due to the interaction of K_2NbF_7 with NbO_2 and NbO, oxofluoride Nb(V) and fluoride Nb(IV) complexes form simultaneously in the KCl–NaCl melt. Thus, the content of the latter increase until the molar ratios in the melt become $NbO_{2\ dissolv.} : K_2NbF_{7\ init.} = 1 : 2$ and $NbO_{dissolv.} : K_2NbF_{7\ init.} = 1 : 3$ and decrease with further dissolution of oxides in the melt. Dissolution of lower niobium oxides in melts containing oxofluoride Nb(V) complexes was also studied.

1. Introduction

The aim of this work was to study the oxidation–reduction processes in melts widely used for electrowinning and refining of refractory metals whose halide and oxohalide complexes generally coexist in these melts [1, 2]. The composition of cathode products formed during electrolysis depends substantially on the composition of these complexes and on their ratio in the molten electrolyte. It is also noteworthy that fluorochloride melts containing dissolved niobium oxides and oxofluorides are of particular interest because of the recent electrochemical synthesis of previously unknown niobium compounds [3].

Earlier studies on oxidation-reduction processes in niobium containing halide and oxohalide melts were focused predominantly on purely electrochemical aspects of their reduction and oxidation, that is, on the processes occurring at the electrode surface [4–18]. The chemical transformations occurring in the melt were mainly of interest when niobium was in its highest oxidation state (Nb(V)) [19–26]. Thus, the great variety of chemical processes involving change in the niobium oxidation state in the melt, as well as those where niobium was initially low valent, were seldom considered in previously published work apart from experimental studies of the stability of the Nb(V) complexes and their spontaneous reduction to Nb(IV) in halide melts [27, 28], as well as the work of Christensen et al. [2] in which the average niobium oxidation number after chemical reaction between Nb(V) and niobium metal was determined as function of oxide content in the FLINAK–K_2NbF_7 melt, and the existence of a low-valent niobium oxofluoride species Nb(IV) OF_y in such melts was suggested. Unfortunately, this suggestion was not confirmed experimentally.

Thus, the principal aim of the present work was to determinate the complex pattern of chemical interactions

between oxofluoride and fluoride niobium complexes of various oxidation states, niobium oxides and metallic niobium in molten salt media and the role of these interactions in niobium electrowinning and refining.

2. Experimental details

The interaction between halide and oxohalide melts with niobium oxides and metallic niobium was studied by linear sweep voltammetry and the determination of kinetic data, using infrared spectroscopy, scanning electron microscopy, X-ray diffraction, optical crystallography and chemical analyses of the products of interaction.

2.1. *Chemicals; preparations of salts and oxides*

Alkali metal chlorides ('spectrally pure') and fluorides ('chemically pure') were used. To remove residual moisture, the salts were heated under vacuum (2 torr) with a slow stepwise increase in temperature up to 700 °C and were then melted in an argon atmosphere in platinum crucibles, at first separately and then as a mixture with the predeterminated ratio of components.

To study the interaction between molten salts and metallic niobium, high-purity niobium crystals (3–5 mm in length with a specific surface of about 450 $cm^2\ g^{-1}$) obtained by electrorefining of commercial electron-beam melted niobium in the K_2NbF_7–KCl–NaCl melt were used. The electrorefining process has been described in detail [29]. The impurity contents in the refined niobium did not exceed 1 ppm of any element, excluding oxygen (200 ppm), carbon (10 ppm) and iron (8 ppm). High-purity niobium pentoxide was prepared by calcination of this niobium metal in air in a muffle furnace at 900 °C and was also used as the starting product for obtaining lower niobium oxides, potassium fluoroniobate and oxofluoroniobates.

For NbO and NbO_2 preparation, compacted tablets of finely crystalline electrorefined niobium and Nb_2O_5 in appropriate ratios were melted four times in a Hereaus arc furnace at about 2000 °C with a tungsten electrode under an atmosphere of high purity helium. The products were homogenized by annealing at 1000 °C for 72 h in evacuated sealed quartz ampoules with a zirconium getter. Such samples were used only when deviation of x in NbO_x did not exceed ± 0.005 (analysis by high-temperature oxidation to constant weight) and X-ray powder diffraction did not show the presence of other phases.

To produce K_2NbF_7, high-purity Nb_2O_5 was dissolved in chemically pure hydrofluoric acid solution (50 wt%). Precipitation of K_2NbF_7 occured on adding a saturated solution of potassium chloride at 80 °C. The product was filtered, washed with rectified ethanol and dried under vacuum at 70–75 °C. The oxofluoride content in the K_2NbF_7 was determined by X-ray diffraction, optical crystallographic and polarographic analyses and did not exceed 0.5%. Oxofluoroniobate synthesis was performed by melting of K_2NbF_7, Nb_2O_5 and KF in appropriate ratios in a glassy carbon vessel under argon atmosphere.

2.2. *Experimental cells and procedures*

The cell for kinetic studies (Figure 1) consisted of a platinum crucible (25 mm diameter, 35 mm high) containing 20 g of salt. The crucible was mounted in the vertical channel of a massive graphite block to stabilize temperature in the reaction zone, which was placed inside a vessel made of heat resistant steel with a brass water-cooled lid. The vessel was filled with argon,

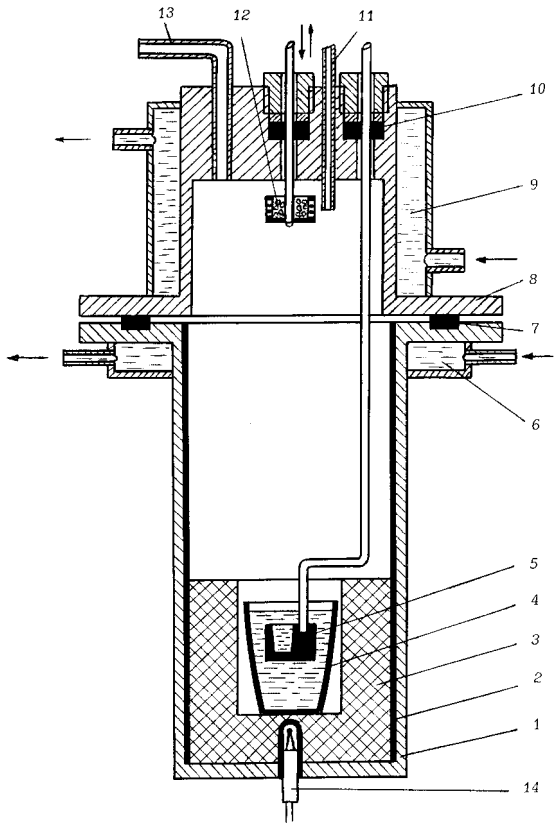

Fig. 1. Cell for study of solubility of niobium and its oxides in halide and oxohalide melts: (1) heat resistant steel vessel; (2) molybdenum lining; (3) graphite block; (4) platinum crucible with molten salt; (5) molybdenum sampler; (6) water cooling of the vessel; (7) Teflon O-ring; (8) brass lid; (9) water jacket of the lid; (10) Wilson gland; (11) argon inlet; (12) molybdenum cup with reactants; (13) vacuum/argon outlet; (14) Pt–PtRh thermocouple.

purified by passing through a heated quartz tube (800 °C) containing titanium sponge. Heating of the experimental cell was carried out in a shaft furnace with silite heaters; the temperature controlling were accurate to ±2 °C.

Crystals of electrolytic niobium, coarse crystalline niobium pentoxide powder or lumps of niobium lower oxides (2–3 mm across) were placed in a molybdenum cup (20 mm diameter, 15 mm high) with walls perforated with 1.5 mm diameter holes. This was immersed in the melt after the preset temperature had been attained in the reaction zone. This cup was screwed to a molybdenum rod of 5 mm diameter, which extended through a gland in the centre of the vessel lid and was connected to a stirring mechanism with vertical reciprocating motion of 15 mm amplitude. It was established earlier [30], that molybdenum was inert to the melts under study in the presence of niobium and its oxides. The mass of niobium or niobium oxide taken exceeded the possible change, caused by its interaction with the melt, by a factor of 5–6. This change was roughly evaluated in preliminary experiments. When the predetermined time of the contact between niobium or its oxide with the melt was completed, the molybdenum cup was lifted out of the melt by the rod to a water-cooled chamber in the vessel lid, and a molybdenum sampler was immersed in the melt for some seconds. The melt sample taken was rapidly cooled in the same chamber by contact with a powerful argon jet. The solid reaction products in this sample and the unreacted residue of materials in the molybdenum cup, were washed free of entrapped salt phase with 10% hydrochloric acid and then washed with distilled water and ethanol. After drying at 40–50 °C they were weighed with an accuracy of 0.0001 g and analyzed for oxygen content by the mass spectrometric method with an accuracy of ±20%, by vacuum extraction (Baltzers EA-1) with an accuracy of ±30% and by high temperature oxidation to constant weight (for concentration of up to 0.1 wt %). The small content of other impurities in the electrorefined niobium ensured a high accuracy (±0.2%) for the latter method. The products in the molybdenum cup, as well as the salt samples taken, were also analyzed by X-ray diffraction with a DRON-3 diffractometer. The total niobium content and the tetravalent niobium concentration in the salt sample were determined by the procedure used earlier [29] with accuracies ±5 and ±1%, respectively. The weight loss of material in the cup, as a result of its dissolution in the melt in a given time, was used to construct the kinetic plots.

Voltammetric measurements were conducted with a three-electrode unit in a glassy carbon cell whose walls were the auxiliary electrode. Working electrodes of glassy carbon, platinum and tungsten were used. The potentials were measured relative to a silver reference electrode (Ag/NaCl–KCl–AgCl 2 wt %). The design of both the electrochemical cell and the reference electrode have been described in detail [31].

3. Results and discussion

3.1. *Interaction of Nb(V) fluoride–chloride melts with Nb_2O_5*

This interaction is the simplest since it is the only one of those considered that does not involved change of oxidation state of the participating components. Nevertheless, a considerable number of compounds belonging to the ternary reciprocal system of K, Nb(V)//F, O may form [1]. Their compositions depend on the $Nb_2O_5 : K_2NbF_7$ and $F^- : K_2NbF_7$ molar ratios in the melt (here F^- are the free fluorine anions, that is, not bonded in the NbF_7^{2-} complex). In this investigation we did not use melts where the molar ratio of $Nb_2O_5 : K_2NbF_7$ exceeds 1 : 3, that is, the regions of formation of di- and trioxofluoride Nb(V) complexes or of potassium metaniobate [11], since such molten salts are of no great importance for practical electrolysis. When the $Nb_2O_5 : K_2NbF_7$ ratio in the melt was 1 : 3 or less, the products of interaction were limited to niobium monooxofluoride complexes, probably according to the reactions:

$$3\,NbF_7^{2-} + Nb_2O_5 = 4\,NbOF_4^- + NbOF_5^{2-} \quad (1)$$

$$3\,NbF_7^{2-} + Nb_2O_5 + 4\,F^- = 5\,NbOF_5^{2-} \quad (2)$$

$$3\,NbF_7^{2-} + Nb_2O_5 + 9\,F^- = 5\,NbOF_6^{3-} \quad (3)$$

These reactions should be considered as plausible although the presence of appropriate compounds, $KNbOF_4$, K_2NbOF_5 or K_3NbOF_6 [21, 25, 32–36] in the final products were corroborated by the analysis of quenched samples of salt mixes. The electrochemical properties of monooxofluoride melts indicated that niobium electroreduction is not sensitively dependent on the actual reaction. The introduction of niobium pentoxide to the K_2NbF_7–KCl–NaCl melt (Figure 2(a)) both with and without KF decreased the height of peaks I and II in the integral voltammetric curves. These peaks corresponded to the reduction of complex fluoride or fluoride–chloride Nb(V) ions to Nb(IV) at $E = -0.63$ V and Nb(IV) discharge to elementary niobium at $E = -1.23$ V [36] respectively. At the same time, peak III, corresponding to the one-step process of monoxo-

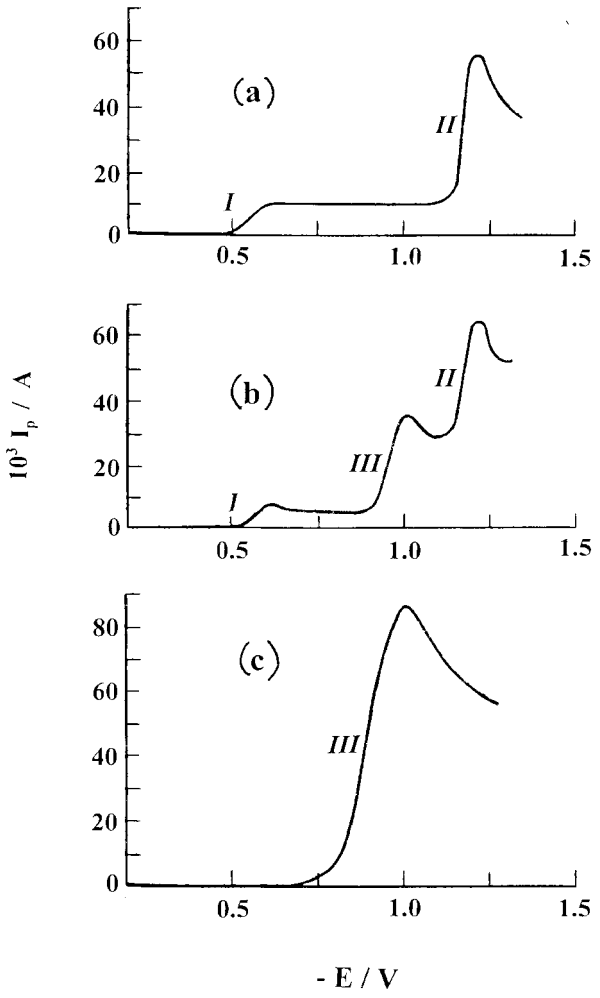

Fig. 2. Linear sweep voltammograms of molten K_2NbF_7–KCl–NaCl with different contents of dissolved Nb_2O_5. Mole ratio Nb_2O_5 : K_2NbF_7 of (a) 0, (b) 1 : 6 and (c) 1 : 3. $C_{K_2NbF_7} = 1.02 \times 10^{-4}$ mol cm^{-3}; $T = 1023$ K; cathodic area, $S = 0.142$ cm^2; potential sweep rate, $v = 0.66$ V s^{-1}.

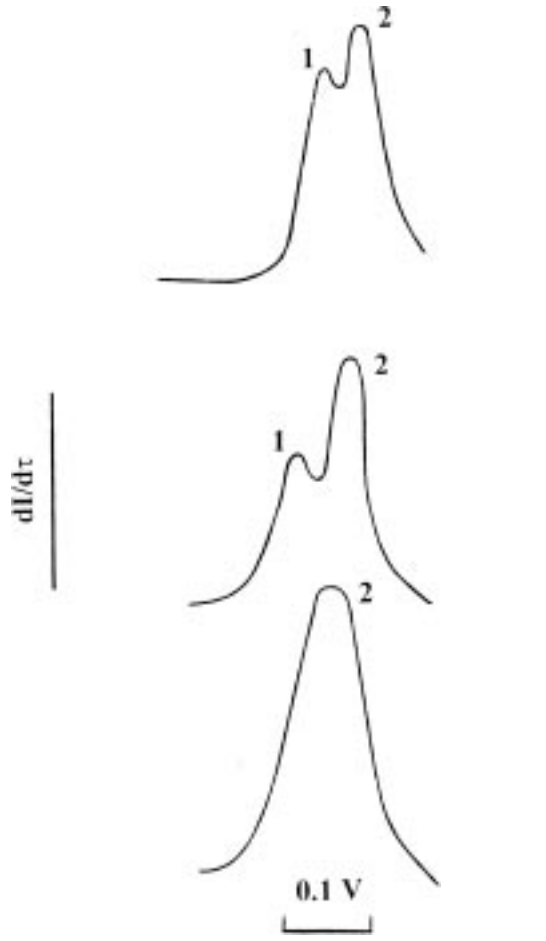

Fig. 3. Change in the shape of differential linear voltammogram of the K_2NbF_7–Nb_2O_5–KCl–NaCl melt with addition of potassium fluoride. Mole ratio KF : Nb_2O_5 of (a) 0, (b) 1 : 2 and (c) $\geqslant$ 1 : 4. Experimental conditions are the same as indicated in Fig. 2.

fluoride complex reduction [11], appeared at a potential close to −1.0 V (Figure 2(b)). As the molar ratio Nb_2O_5 : K_2NbF_7 = 1 : 3 was attained, that is, when the melt did not contain any oxygen-free fluoride complexes, this peak became the only one in the integral voltammogram (Figure 2(c)). The presence (according to reaction (1)) of two monoxofluoride complexes simultaneously in the K_2NbF_7–KCl–NaCl—Nb_2O_5 melt was shown by two distinct peaks in the differential voltammetric curve, the first peak being approximately four times higher than the second (Figure 3(a)), thus, the first peak may be attributed to the $NbOF_4^-$ complex.

The introduction of fluorine anions into the melt resulted in a gradual decrease in the height of this peak and in a growth of the second one (Figure 3(b)). As a KF concentration ration corresponding to the stoichiometry of Reaction 2, was attained, the differential voltammetric curved showed only one peak (Figure 3(c)) corresponding to the discharge of $NbOF_5^{2-}$ complexes. Narrow absorption bands appeared in the infrared spectra in the 920 cm^{-1} region, attributed to terminal Nb–O bonds [35]. As the fluorine ion concentration was further increased, the formation of $NbOF_6^{3-}$ complexes did not cause the appearance of discrete waves corresponding to their discharge in any of the voltammograms. Only a minor shift of the potential to negative values (several tens of millivolts) was observed.

Thus, though the discharge potentials of niobium oxofluoride complexes became somewhat more negative as the fluoride content in the melt increased, they remained more positive by 0.1–0.15 V than the discharge of oxygen-free halide complexes [36].

3.2. *Interaction of Nb(V) fluoride–chloride melts with NbO_2*

Niobium dioxide interacted actively with melts of the K_2NbF_7–KCl–NaCl system. Figure 4(a) shows the change in quantity of dissolved NbO_2 (from the loss of weight of NbO_2 specimen) against time in a molten equimolar mix of KCl–NaCl with 30 wt % of K_2NbF_7, at 750 °C and Figure 4(b) illustrates the related change in the proportion of Nb(IV) in the melt samples. Each of the curves consists of two branches separated by a bend and by a sharp maximum, respectively. The positions of the bend and maximum on the abscissa coincide. The left hand branches of the curves show a greater rate of niobium dioxide dissolution in the melt along with a greater rate of increase in Nb(IV) concentration in the first stage of interaction to a maximum value which is 1/3 of the total niobium content in the melt. At the same time curve 1 (Figure 5), plotted on the base of the same experimental data, shows that, for the entire period, the molar ratio between the quantity of the NbO_2 dissolved in the melt and the quantity of Nb(IV) formed thereby

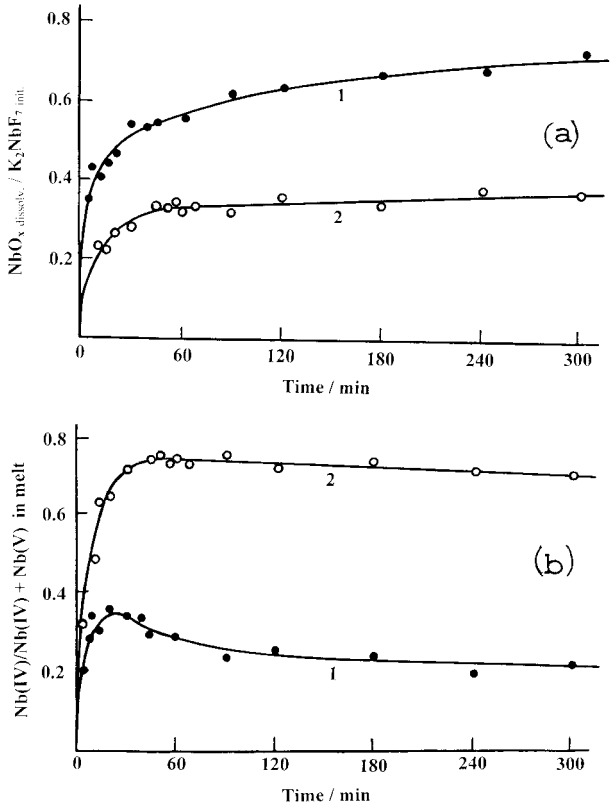

Fig. 4. Amount of dissolved niobium lower oxide (moles per one mole of initial amount of K_2NbF_7) (a) and the relative proportion of Nb(IV) in the melt (b) against time during interaction of NbO_2 (1) and NbO (2) with the K_2NbF_7 30 wt %–KCl–NaCl melt at 750 °C.

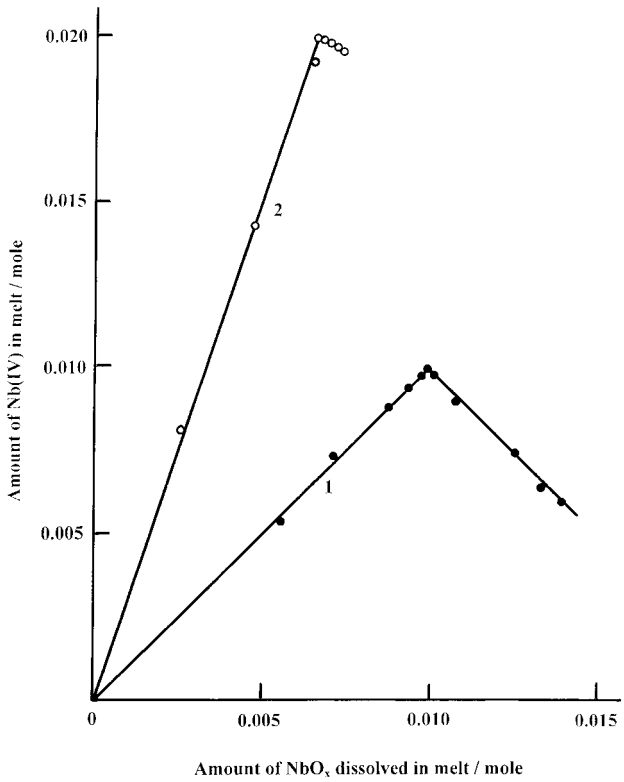

Fig. 5. Molar ratio of the amount of niobium oxide dissolved in the molten K_2NbF_7 30 wt %–KCl–NaCl at 750 °C to the amount of Nb(IV) in the melt: (1) NbO_2 and (2) NbO.

remains constant and equal to 1 : 1. Transition from the first to the second stage, at which the Nb(IV) oxide continues to dissolve in the melt (although at a much reduced rate), but nevertheless the Nb(IV) concentration decreases rather rapidly, occurs when the molar ratio of dissolved NbO_2 to the amount of initial K_2NbF_7 reached 1 : 2 (Figure 4(a), curve 1).

The solid residues after the first stage of dissolution consisted of unreacted NbO_2; however, no solid residue was found when the ratio of initial NbO_2 to K_2NbF_7 (in moles) did not exceed 1 : 2. This fact along with the stability of the $NbO_{2\ dissolv.}$: Nb(IV) molar ratio for all the tests on the first stage suggests that the reactions of the first and the second stages are strictly consecutive. In other words, the reaction of the second stage reaches a noticeable rate only after the completion of the first reaction.

The solid residues formed during the second stage of NbO_2 dissolution contained NbO, which covers the surface of the NbO_2 lumps with a dense crust (Figure 6). Apparently, the formation of this crust, almost impervious to the melt, is responsible for the gradual slow down of the second stage reaction. This is supported by

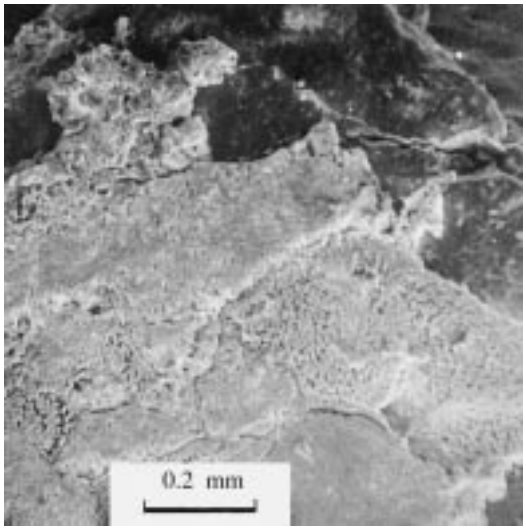

Fig. 6. SEM micrograph of the surface of an NbO_2 lump covered partially with NbO crust after 3 h contact with the K_2NbF_7 30 wt %–KCl–NaCl melt at 750 °C (a part of initial fresh surface of NbO_2, which has been screened by an other NbO_2 lump in the course of experiment, can be seen at the top of the photograph).

the fact that, in additional tests when partially reacted NbO_2 was substituted for fresh niobium(IV) oxide, the process of the second stage continued to a significantly greater decrease of Nb(IV) concentration, for example, Nb(IV) : Nb(IV) + Nb(V) = 0.01 at τ = 5 h with four changes of the NbO_2 charges against 0.23 for one charge used.

The introduction of niobium dioxide to the K_2NbF_7–KCl–NaCl melt changed its voltammogram (Figure 7(a)): wave I shifted to the anodic region (Figure 7(b)) due to the appearance of low-valent niobium ions in the melt. The ratio of the values of anodic and cathodic currents of the first wave became proportional to the ratio of concentrations of Nb(IV) and Nb(V) fluoride complexes in the melt.

Simultaneously, a new wave III analogous to wave III in Figure 2(b) appeared at a peak potential of −1.0 V. This may be caused by the formation of Nb(V) oxofluoride complexes. On attaining the ratio $NbO_{2\ \text{dissolv.}}$: $K_2NbF_{7\ \text{init.}}$ = 1 : 2 (the maximum on curve 1 in Figure 4(b)) wave I shifts completely to the anodic region, thus being transformed from a reduction wave $Nb(V) + e^- \rightarrow Nb(IV)$ to an oxidation wave $Nb(IV) - e^- \rightarrow Nb(IV)$. So, from this point, the melt contained no initial Nb(V) fluoride complexes, but only the complexes formed from the interaction of the melt with NbO_2, that is, Nb(IV) fluoride and Nb(V) oxofluoride complexes (Figure 7(c)). The decrease in the concentration of the former and a simultaneous increase in the concentration of the latter with further NbO_2 dissolution (the descending branch of the curve 1 in Figure 4(b)) manifest themselves on voltammograms as a growth of wave III and a decrease in waves I and II (Figure 7(d)).

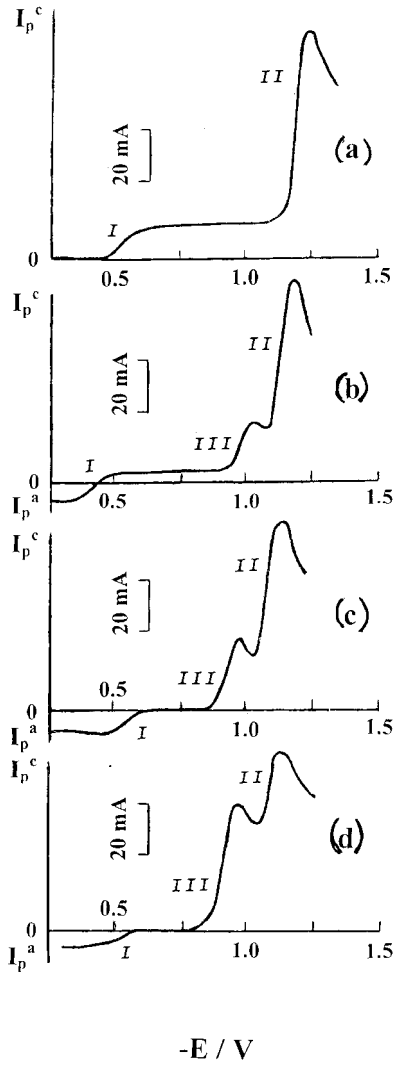

Fig. 7. Linear sweep voltammograms of the molten K_2NbF_7–KCl–NaCl with different contents of dissolved NbO_2. Mole ratio $NbO_{2\ \text{dissolv.}}$: $K_2NbF_{7\ \text{init.}}$ of (a) 0, (b) 0.25, (c) 0.5 and (d) 0.7. $C_{K_2NbF_7} = 1.60 \times 10^{-4}$ mol cm^{-3}; T = 1073 K; S = 0.137 cm^2; v = 0.5 V s^{-1}.

Thus, niobium dioxide dissolving in the K_2NbF_7–KCl–NaCl melt interacts with it in two successive stages. At the first state Nb(IV) fluorocomplexes form, and, at the second stage, they are oxidized to oxofluoride Nb(V) ions. Apparently, the reactions are as follows:
When $NbO_{2\ \text{dissolv.}}$: $K_2NbF_{7\ \text{init.}} \leqslant 1 : 2$,

$$2\,NbF_7^{2-} + NbO_2 \rightleftharpoons NbF_5^- + 2\,NbOF_4^- + F^- \qquad (4)$$

When $NbO_{2\ dissolv.} : K_2NbF_{7\ init.} > 1 : 2$,

$$3\,NbF_5^- + 3\,NbO_2 + F^- \rightleftharpoons 4\,NbOF_4^- + 2\,NbO \quad (5)$$

The designation $NbO_{x\ dissolv.}$ ($x = 1$ or 2), indicates the loss of weight of oxide contained in the molybdenum cup here and throughout the paper, including Figures 4, 5, 8, 9.

The equilibrium of Reaction 4 is virtually completely shifted to the right, and Reaction 5 is hindered by the solid product formed and by the diffusion of NbF_5^- and F^- into the bulk melt. It may be assumed that Reaction 5 describes the entire process based on disproportionation of complex Nb(IV) ions in the melt according to the reaction:

$$5\,NbF_5^- + 3\,F^- \rightleftharpoons 4\,NbF_7^{2-} + Nb^0 \quad (6)$$

In oxygen-free chloride–fluoride melts, the validity of Reaction 6 was established earlier [29]. However, in these melts, this reaction was not substantially developed, particularly when the melt was in contact with metallic niobium (as in cells for electrolytical refining and electroplating). Apparently, an excess of niobium dioxide in the reaction system promotes a shift of equilibrium (Reaction 6) to the right as a result of NbO_2 interaction with its products by the reactions:

$$Nb^0 + NbO_2 \rightleftharpoons 2\,NbO \quad (7)$$

and (4). It is clear that Reactions 6, 7 and 4 give the same total reaction (i.e. Reaction 5).

3.3. *Interaction of Nb(V) fluoride–chloride melts with NbO*

The oxidation–reduction processes in the K_2NbF_7–KCl–NaCl melt involving niobium monoxide are similar to those during niobium dioxide dissolution. In both cases there are two stages of interaction, however, the 'oxidizing' power of niobium(II) oxide is much weaker than that of niobium(IV) oxide and hence the 'reducing' function of NbO is more evident. This is clearly indicated by a significant decrease in the rate of Nb(IV) oxidation in the second stage of dissolution in transition from NbO_2 to NbO (Figure 4(b)). Moreover, the proportion of Nb(IV) to total niobium a the maximum point increases to 0.75 in the case of NbO dissolution. This occurs at the molar ratio $NbO_{dissolv.} : K_2NbF_{7\ init.} = 1 : 3$.

Figure 5 (curve 2) shows that, for the entire first stage of NbO dissolution the NbO : Nb(IV) molar ratio remains constant, indicating the formation of three moles of Nb(IV) upon dissolution of one mole of NbO.

As in the case of NbO_2, a second phase appears in the solid residue after NbO dissolution only at the second stage of the interaction, but in this case it is a very small amount of finely dispersed metallic niobium.

The voltammograms of the K_2NbF_7–KCl–NaCl melt after addition of NbO show the same qualitative patterns at both stages of interaction, as those observed after the addition of NbO_2, differing in the height of the peaks as well as by a minor negative shift of peak III at the first stage. The shape of the differential voltammograms after the second stage of NbO dissolution suggests the presence of oxofluoride complexes of two types, presumably $NbOF_4^-$ and $NbOF_6^{3-}$. Because of the complex composition of the corresponding salt samples, we have failed to definitely interpret their X-ray and infrared spectra, but the differences in the phase compositions of fluoride–chloride melts after dissolution of NbO_2 and NbO are seen.

The data suggest that niobium monooxide dissolution in the K_2NbF_7–KCl–NaCl melt is described by the following reactions in two successive stages:
When $NbO_{dissolv.} : K_2NbF_{7\,init.} \leqslant 1 : 3$,

$$3\,NbF_7^{2-} + NbO \rightleftharpoons 3\,NbF_5^- + NbOF_6^{3-} \quad (8)$$

When $NbO_{dissolv.} : K_2NbF_{7\,init.} > 1 : 3$

$$3\,NbF_5^- + 4\,NbO + F^- \rightleftharpoons 4\,NbOF_4^- + 3\,Nb^0 \quad (9)$$

In this case, Reaction 8 proceeds more rapidly and practically completely, whereas the rate of oxidation of Nb(IV) ions with excess NbO (Reaction 9) is rather slow.

3.4. *Interaction of Nb(V) oxofluoride–chloride melts with NbO_2 and NbO*

During the electrolysis of oxohalide–halide niobium melts, lower niobium oxides may be electrodeposited [1–3, 10, 18, 38] on the cathode, and, being in contact with the melt, can interact with it. NbO_2 and NbO are also formed as a result of the interaction of melts containing niobium oxohalides with metallic niobium wich is both the cathode product and the anodic material [39]. Therefore, it seemed of interest to study the processes of lower niobium oxide dissolution in these melts.

Figure 8 represents the kinetic curves for the interaction of the K_2NbF_7–Nb_2O_5–KCl–NaCl melt (of molar ratio $K_2NbF_7 : Nb_2O_5 = 3 : 1$) with NbO_2. As in the case of a melt without Nb_2O_5, this interaction occured in two stages but at a much lower rate of Nb(IV) ion oxidation in the second stage. However, the principal difference of NbO_2 dissolution in oxofluoride–chloride melt from its dissolution in an oxygen free melt, is a

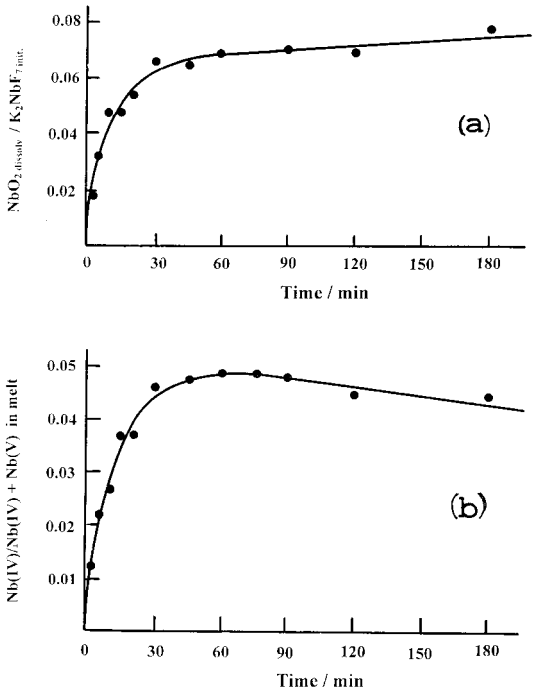

Fig. 8. Amount of dissolved NbO_2 (moles per one mole of initial quantity of K_2NbF_7) (a) and the relative proportion of Nb(IV) in the melt (b) against time during interaction of NbO_2 with the K_2NbF_7 30 wt %–Nb_2O_5–KCl–NaCl melt at 750 °C. Mole ratio K_2NbF_7 : Nb_2O_5 = 3 : 1.

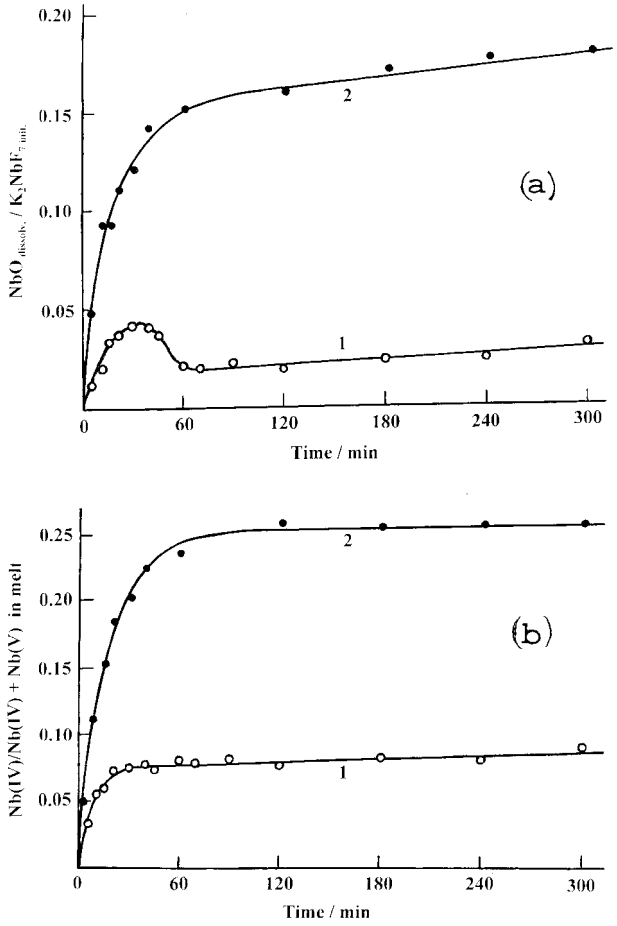

Fig. 9. Amount of dissolved NbO (moles per one mole of initial quantity of K_2NbF_7) (a) and the relative proportion of Nb(IV) in the melt (b) against time during interaction of NbO with the K_2NbF_7 30 wt %–Nb_2O_5–KCl–NaCl (1) and K_2NbF_7 30 wt %–Nb_2O_5–LiF–NaF–KF (2) melts at 750 °C. Mole ratio K_2NbF_7 : Nb_2O_5 = 3 : 1.

rather small share of lower oxidation state niobium, for example, at the maximum in the curve (Figure 8(b)), Nb(IV) : Nb(IV) + Nb(V) = 0.05 only. This corresponded to molar ratios $NbO_{2\ dissolv.}$: Nb(IV) = 4 : 5 and $NbO_{2\ dissolv.}$: $K_2NbF_{7\ init.}$ = 1 : 15. It is difficult to use these empirical ratios for writing equations for NbO_2 interaction with the chloride–fluoride melt. It is conceivable that, in this case, there are several simultaneously redox reactions at each step of NbO_2 dissolution.

During the interaction of a K_2NbF_7–Nb_2O_5–KCl–NaCl melt (molar ratio K_2NbF_7 : Nb_2O_5 = 3 : 1) with NbO (Figure 9(a)) the stage of Nb(IV) oxidation is probably absent, in contrast to the earlier cases of lower niobium oxide dissolution. At the same time, the curve describing the relationship between the mass of oxide dissolved in the melt and the dissolution time (Figure 9(a), curve 1) has the most complex shape. Three sections are clearly seen in this curve.

The first section corresponds to the formation of a liquid phase product. This is indicated not only by the decrease in mass of the NbO sample but also by the relatively high rate of Nb(V) to Nb(IV) reduction at this stage of dissolution and by the absence of a solid product after experiments without excess NbO. For the entire first stage of NbO dissolution, the molar ratio NbO : Nb(IV) was constant (1 : 3.3). This stage terminated at the ratio of $NbO_{dissolv.}$: $K_2NbF_{7\ init.}$ = 1 : 25.

Increase in the weight of solid and a lower rate of niobium reduction in the second stage is probably due to a transition to the formation of a solid reaction product of reaction at the NbO surface. This product is identified by X-ray phase analysis as NbO_2.

We suggest that the melt at the third stage generally interacts, not with the initial NbO, but with NbO_2 formed in the second stage. The process is accompanied by a small decrease in the weight of solid and occurs at a rather low rate of Nb(V) reduction. The highest degree of reduction of the oxofluoride–chloride melt with niobium monoxide, (Nb(IV) : Nb(IV) + Nb(V) = 0.07, obtained by reduction for 6 h at 750 °C, is significantly

lower than that attained at the first stage of NbO dissolution in the fluoride–chloride oxygen-free melt. Figure 9 (curves 2(a) and 2(b)) indicates that the degree of reduction of Nb(V) to Nb(IV) may be increased several times with simultaneous transition to a simpler NbO dissolution, when the chloride mixture is replaced by a fluoride mixture (FLINAK). This effect is caused by the fact that fluoride melt dissolves more solid products from the sample surface than the chloride–fluoride melt.

4. Conclusion

The Nb(V) fluoride–chloride melts interact actively with all three niobium oxides. The composition of complexes formed during Nb_2O_5 dissolution depends on the molar ratios Nb_2O_5 : K_2NbF_7 and F^- : Nb_2O_5. When Nb_2O_5 : K_2NbF_7 = 1 : 3 and less, the formation of three monooxofluoride complexes ($NbOF_4^-$, $NbOF_5^{2-}$, or $NbOF_6^{3-}$) is possible, probably depending on the availability of free F^- ions in the melt. The presence of any of these ions is characterized by the appearance of a wave with the peak at a potential close to −1.0 V vs Ag/Ag^+ on the voltammograms (i.e., more positive than the potential of Nb(IV) ion discharge to niobium metal).

The interaction of fluoride–chloride Nb(V) melts with lower niobium oxides occurrs in two successive stages. At the first stage Nb(IV) ions are formed and their concentration grows strictly proportionally to the increase in the oxide content. The observed voltammetric curves, infrared spectroscopy and X-ray diffraction do not give reliable proof of the formation of Nb(IV) oxofluoride complexes. Apparently, as a result of lower oxide dissolution, oxygen-free Nb(IV) complexes are formed, and oxygen appears in the monoxofluoride Nb(V) complexes, formed simultaneously, with the concentration of the latter increasing proportionally with the increase of the oxide. At the same time, the concentration of the initial fluoride complex NbF_7^{2-} fails and reaches zero by the end of the first stage.

In the second stage, as niobium oxide is further dissolved, the oxofluoride complex concentration increases further, but the Nb(IV) concentration decreases (this occurs more extensively in the case of NbO_2). Apparently, the latter process involves disproportionation and is accompanied by the formation of solid products such as NbO and Nb due to the dissolution of NbO_2 and NbO, respectively. The maxima in the [Nb(IV) : Nb(IV) + Nb(V)] against time curves separate the stages and occur at the molar ratios given in Table 1.

The time dependencies of NbO_2 interaction with oxofluoro–chloride melts are analogous in form to those observed for NbO_2 interaction with fluoro-chloride melts (which is due to a two stage process), but are characterized by a relatively smaller maximum degree of niobium reduction. The NbO interaction with these melts occurs in three stages with increase in Nb(IV) concentration at all the stages. The chemical nature of these interactions is complex and not completely understood.

Table 1.

Molar ratios	NbO_2	NbO
Nb(IV) : Nb(IV) + Nb(V)	1 : 3	3 : 4
$NbO_{x\ \text{dissolv.}}$: $K_2NbF_{7\ \text{init.}}$	1 : 2	1 : 3
$NbO_{x\ \text{dissolv.}}$: Nb(IV)	1 : 1	1 : 3
Nb(IV) : $K_2NbF_{7\ \text{init.}}$	1 : 2	1 : 1

Acknowledgements

The authors are grateful to Professor D.H. Kerridge for criticism and valuable discussion. They gratefully acknowledge the financial support of RFBR (grant 98-03-32804).

References

1. V.I. Konstantinov, 'Electrolytic obtaining of tantalum, niobium and their alloys', Metallurgiya, Moscow (1977).
2. E. Christensen, Xindong Wang, J.H. von Barner, T. Ostvold and N.J. Bjerrum, *J. Electrochem. Soc.* **141** (1994) 1212.
3. V.V. Grinevitch, M.S. Model, O.G. Karpinsky, A.V. Arakcheeva, S.A. Kuznetsov and E.G. Polyakov, *Dok1. Akad. Nauk USSR* **319** (1991) 389.
4. L.E. Ivanovsky and M.T. Krasilnikov, *Trans. Inst. Electrochem. Ural Branch Ac. Sci. USSR* **1** (1960) 49.
5. L.E. Ivanovsky, I.G. Rozanov, M.T. Krasilnikov and A.F. Plekhanov, *Trans. Inst. Electrochem. Ural Branch Ac. Sci. USSR* **5** (1964) 111.
6. M.T. Krasilnikov and L.E. Ivanovsky, *Trans. Inst. Electrochem. Ural Branch Ac. Sci. USSR* **17** (1971) 94.
7. M.T. Krasilnikov and L.E. Ivanovsky, *Trans. Inst. Electrochem. Ural Branch Ac. Sci. USSR* **17** (1971) 98.
8. S. Senderoff and G.W. Mellors, *J. Electrochem. Soc.* **113** (1966) 66.
9. M. Sakava and T. Kuroda, *Denki Kagaku.* **36** (1968) 653.
10. M. Chemla and V. Grinevitch, *Bull. Soc. Chim. France*, N 3 (1973) 853.
11. V.I. Konstantinov, E.G. Polyakov and P.T. Stangrit, *Electrochim. Acta* **26** (1981) 445.
12. Q. Zhiyu and P. Taxil, *J. Appl. Electrochem.* **15** (1985) 259.
13. G.P. Capsimalis, E.S. Chen and R.E. Peterson, *J. Appl. Electrochem.* **17** (1987) 253.
14. L. Arurault, J. Bouteillon, J. de Lepinay, A. Khalidi and J.C. Poignet, Proceedings of the Third International Symposium on 'Molten Salt Chemistry and Technology', Paris (1991), p. 305.
15. A. Barhoun, F. Lantelme, M.E. de Roy and J.P. Besse, Proceedings of the Third International Symposium on 'Molten Salt Chemistry and Technology', Paris (1991), p. 313.

16. A. Khalidi, P. Taxil, B. Lafage and A.P. Lamaze, Proceedings of the Third International Symposium on 'Molten Salt Chemistry and Technology', Paris (1991), p. 421.
17. A. Barhoun, Y. Berghoute and F. Lantelme, *J. Alloys Compd.* **179** (1992) 241.
18. F. Lantelme, Y. Berghoute, J.H. von Barner and G.S. Picard, *J. Electrochem. Soc.* **142** (1995) 4097.
19. Yu. A. Buslayev, R.L. Davidovich and V.A. Bochkariova, *Izv. AN USSR. Neorg. Mater.* **1** (1965) 483.
20. I. Koltsov, *AN USSR. Neorg. Mater.* **1** (1965) 907.
21. A.I. Agulyansky, V.A. Bessonova and V.Ya. Kuznetsov, *AN USSR. Neorg. Mater.* **20** (1984) 1207.
22. J.S. Fordyce and R.L. Baum, *J. Chem. Phys.* **44** (1966) 1166.
23. A.A. Kazayn, T.V. Afanasyev and V.F. Lomovtsev, *Trans. Giredmet.* **74** (1977) 41.
24. V.Ya. Kuznetsov, D.L. Rogachiov, A.I. Agulyansky and V.T. Kalinnikov, *Zh. Struct. Chim.* **26** (1985) 85.
25. A.I. Agulyansky, E.L. Tikhomirova and V.T. Kalinnikov *Zh. Neorg. Chim.* **33** (1998) 1155.
26. J.H. von Barner, E. Christensen, N.J. Bjerrum and B. Gilbert, *Inorg. Chem.* **30** (1991) 561.
27. Z. Alimova, E. Polyakov, L. Polyakova and V. Kremenetsky, *J. Fluor. Chem.* **59** (1992) 203.
28. L. Arurault, J. Bouteillon and J. Poignet, *J. Electrochem. Soc.* **142** (1995) 16.
29. V.V. Grinevitch, V.A. Reznichenko, G.A. Menyailova and Yu. I. Bykovskaia, *in* 'Processes of Production and refining of Refractory Metals', Nauka, Moscow (1975) p. 220.
30. V.V. Grinevitch and V.A. Reznichenko, *in* 'Metallurgy of Tungsten, Molybdenum and Niobium', Nauka, Moscow (1967), p. 177.
31. L.P. Polyakova, E.G. Polyakov, A.I. Sorokin and P.T. Stangrit, *J. Appl. Electrochem.* **22** (1992) 628.
32. A.E. Baker and H.M. Haendler, *Inorg. Chem.* **1** (1962) 127.
33. D.L. Davidovitch, T.A. Kaydalova, T.F. Levshina and V.I. Serguiyenko, 'Atlas of Infrared Absorption Spectra and X-radiography Data of Complex Fluorides of Metals of IV and V Groups', Nauka, Moscow (1972).
34. A.I. Agulyansky, E.L. Tikhomirova, V. Ya. Kuznetsov and V.T. Kalinnikov, *Zh. Neorg. Chim.* **33** (1988) 85.
35. D.V. Pikayeva, A.I. Agulyansky, Yu.I. Balabanov and V.T. Kalinnikov, *Zh. Neorg. Chim.* **34** (1989) 3046.
36. S.A. Kuznetsov, A.L. Glagolevskaya, V.V. Grinevitch and P.T. Stangrit, *Electrokhimiya* **28** (1992) 1344.
37. R. Stromberg, *Acta Chem. Scand.* **A38** (1984) 603.
38. M.M. Wong and D.E. Kirby, *Electrochem. Technol.* **6** (1968) 119.
39. V.V. Grinevitch, V.A. Reznichenko, M.S. Model, S.A. Kuznetsov and E.G. Polyakov, Third International Symposium, *Op. cit* [14], Abstr. 22(3).